Separation Science and Technology
Publication details, including instructions for authors and subscription information:
http://www.informaworld.com/smpp/title~content=t713708471

Flux Enhancement in a Helical Microfiltration Module with Gas Injection

Kun Yong Chung[a]; Min Soo Lee[a]
[a] Department of Chemical Engineering, Seoul National University of Technology, Nowon, Seoul, Korea

To cite this Article Chung, Kun Yong and Lee, Min Soo(2005) 'Flux Enhancement in a Helical Microfiltration Module with Gas Injection', Separation Science and Technology, 40: 12, 2479 — 2495
To link to this Article: DOI: 10.1080/01496390500267533
URL: http://dx.doi.org/10.1080/01496390500267533

Separation Science and Technology, 40: 2479–2495, 2005

ISSN 0149-6395 print/1520-5754 online
DOI: 10.1080/01496390500267533

Flux Enhancement in a Helical Microfiltration Module with Gas Injection

Kun Yong Chung and Min Soo Lee
Department of Chemical Engineering, Seoul National University of Technology, Nowon, Seoul, Korea

Abstract: A helical flow module with an inner rod mounted membrane was designed and built to reduce gel layer deposit and membrane fouling during microfiltration. Controlled centrifugal instabilities resulting from flow in a helically grooved channel, as well as the leakage flow between adjacent grooves, generated secondary vortex flows. The permeation fluxes for helical modules with Dean vortex flow were compared with flat crossflow modules at different operating pressures, concentrations, and feed flow rates. The permeation flux of the helical module for a feed solution containing 0.3 wt% kaolin solution at 1.2 bar was 57% higher than that of the flat module. Moreover, in addition to secondary vortex flow, compressed air was introduced to the membrane module. The increase in flux for the helical module with air injection was significant: the flux enhancements at 1.3 bar, 2 L-solution/min and 1.3 L-air/min for 0.1 wt% solutions of kaolin and bentonite were 47 and 73%, respectively.

Keywords: Helical module, Dean vortex, turbulent flow, gas-injection, fouling, microfiltration

INTRODUCTION

Pressure-driven membrane processes are widely used in many industrial applications for concentrating and fractionating various components in solutions and suspensions. Although theses processes have become very attractive, the rapid decrease in the permeate flux, which results from membrane

Received 6 October 2004, Accepted 17 May 2005
Address correspondence to Kun Yong Chung, Department of Chemical Engineering, Seoul National University of Technology, Nowon, Seoul 139-743, Korea. Tel.: 82-2-970-6608; Fax: 82-2-977-8317; E-mail: kychung@snut.ac.kr

fouling and concentration polarization, often limits their practical use in industrial applications. Recent research efforts have focused on fundamental aspects of fouling and concentration polarization mechanisms with the goal of minimizing flux decline in pressure-driven membrane applications. Various approaches have been used: (i) treatment to lower the solid concentration in feed streams, (ii) improved methods of operation for controlling the permeation flux and minimizing the transmembrane pressure difference, and (iii) lowering the concentration gradient between the membrane surface and bulk solution (1). The first strategy is of limited use because it is often not a practical solution to the problem. Recent developments in membrane processes for pilot plant commercial applications are based on the approach of maintaining low transmembrane flux; that is, below a "critical flux" where fouling does not occur. This critical flux hypothesis states that on start-up if flux is maintained at a low enough value, the membrane will not foul (2). The last approach includes chemical modification of the membrane surface as well as physical and hydrodynamic methods of minimizing surface fouling. Chemical modification methods, however, require the membrane to be customized for the constituents in each feed stream, which is often a very difficult task to achieve (3). Also, surface treatment has little effect on the behavior of suspended particles once a secondary cake layer has been formed. On the other hand, physical and hydrodynamic techniques to reduce concentration polarization have been shown to be effective in enhancing the permeate flux of ultrafiltration or microfiltration membranes. Some examples of these techniques are: (i) mixing with a static mixer (4, 5) or screw-threaded inserts in tubular modules (6), (ii) cleaning balls in the feed channel (7, 8), (iii) fluidized bed operation with small glass balls in the tubular module (9), (iv) pulsatory flow with a corrugated membrane surface (10–12), (v) the use of rotating disk equipment (13–15), (vi) vibratory shear-enhanced filtration systems (16, 17), and (vii) production of centrifugal instabilities such as Taylor (18–21) and Dean vortices (22–33). Specifically, the Taylor vortex system exhibits excellent flux and rejection characteristics. It is, however, difficult to scale-up, consumes a large amount of energy, and may have long-term sealing problems. In order to overcome the scale-up limitations and sealing problems described above, the Dean vortex membrane system has been investigated. Winzeler and Belfort (22) suggested spirally wound channels of semicircular cross-section which can sweep the membrane surface in a continuous bend. This stack module performed about six-fold better than conventional plate and frame membrane modules with feed solutions containing yeast and whey. Helical hollow fiber or tubular systems using a Dean vortex have also been actively investigated (26–32). Despite these potential benefits, no large-scale membrane modules are commercially available based on the Dean vortex. Recently, it has been reported that the creation of a gas/liquid two-phase flow by injecting gas into the feed effectively reduces concentration polarization. This occurs because the injection of gas into the liquid stream promotes both turbulence

at the surface of membrane and superficial crossflow velocity. Cui et al. (34, 35) and Um et al. (36) have reported up to 320% and 400% enhancement of permeate flux with gas injection into tubular and flat sheet ultrafiltration membrane systems, respectively.

The purpose of this paper is to present the efficiency of a helical flow module with an inner rod mounted membrane. Controlled centrifugal instabilities resulting from flow in helically grooved channels were used to reduce gel layer deposit and membrane fouling during microfiltration. In addition, the leakage flow between adjacent channel grooves may augment secondary vortex flow generated in the helical space by centrifugal force. Finally, compressed air, in addition to secondary vortex flow, was introduced to the membrane module to keep the fluid well-mixed, and thereby reduce the potential of particles to block membrane pores. In this paper, the results obtained for Dean vortex flow and crossflow without vortices as well as gas injection are compared and analyzed.

EXPERIMENTAL

System

The experimental apparatus used in this study is shown schematically in Fig. 1. The system consisted of a 10 L stainless steel reservoir tank (1), a rotary pump (2) (PMR 401138, Korea), a membrane module (4), a compressor (10) (3/4HP-Professional Air Compressor, Namsun Power Tools, Korea), a flowmeter (6) (VFC-151, Dwyer Instruments), and an electronic balance

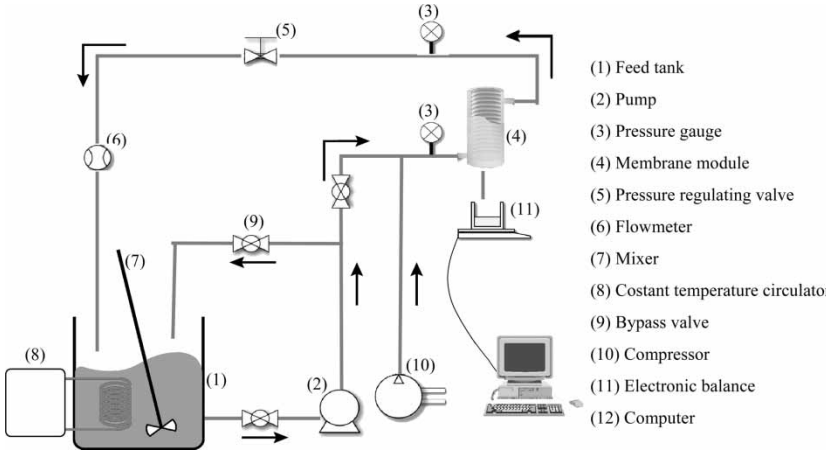

Figure 1. Schematic experimental flow diagram of the microfiltration system equipped with a membrane module.

(11) (HF-6000G, AND) interfaced to a computer to collect permeate flux data. A bypass line with a valve (9) was used to control the flow rate and operating pressure. The inlet and outlet pressures (3) of the module were measured and then the operating pressure was set as the average of these values. The feed flow rate was measured with a flowmeter before the stream was recycled to the tank. The permeate stream was collected in a permeate reservoir, and then periodically recycled to the feed tank in order to maintain an essentially constant feed concentration. The particles in the feed tank were prevented from gravity settling by using a mixer. The temperature of the feed solution was controlled by a cooling coil placed in the feed tank. Compressed air could be injected at the entrance of the module in order to produce turbulent flow in the membrane module. The air flow rate was measured with the drum type gas meter (TG10, Ritter Co.) and maintained at about 1.3 L/min under 1.3 bar.

Materials

The membrane used in this study was a mixed-ester cellulose microfilter (Asypor, Domnick Hunter Ltd.), with a nominal pore size of 0.2 μm. The active area of the membrane was 160 cm^2. Kaolin and bentonite particles were used, and all feed solutions were prepared in ultra-pure water (greater than 18.2 MΩ-cm) produced by a Maxima system (Elga Co.). The particle sizes of kaolin and bentonite were measured with a laser particle analyzer system (Otsuka Co., PAR-III), as shown in Fig. 2.

Membrane Modules

Two microfiltration membrane modules were used to compare the performance obtained in the presence and absence of Dean vortices, as well as the flux enhancement due to gas injection. The membrane modules are shown in Fig. 3. The flat sheet membranes (2) were wrapped around perforated supports (1), arranged coaxially and radially spaced from the cylindrically profiled surface, which was formed with a helical groove (3) or simply flat (4), respectively. The modules were made of transparent acrylic plastic so that the flow pattern could be visualized optically. The fluid to be filtered passed one axial end along the passage defined between the membrane and the profiled surface. The corkscrew-type vortex flow was produced in the existing direction of the helical grooves. A narrow gap between adjacent turns of the grooves and membrane induced leakage flow. Bellhouse (32) reported mathematically the interaction between leakage flow and corkscrew vortex flow within the helical space. The action of the high-velocity leakage flow was to overwhelm the pre-existing upstream corkscrew vortex and reinforce the downstream corkscrew vortex. Hence

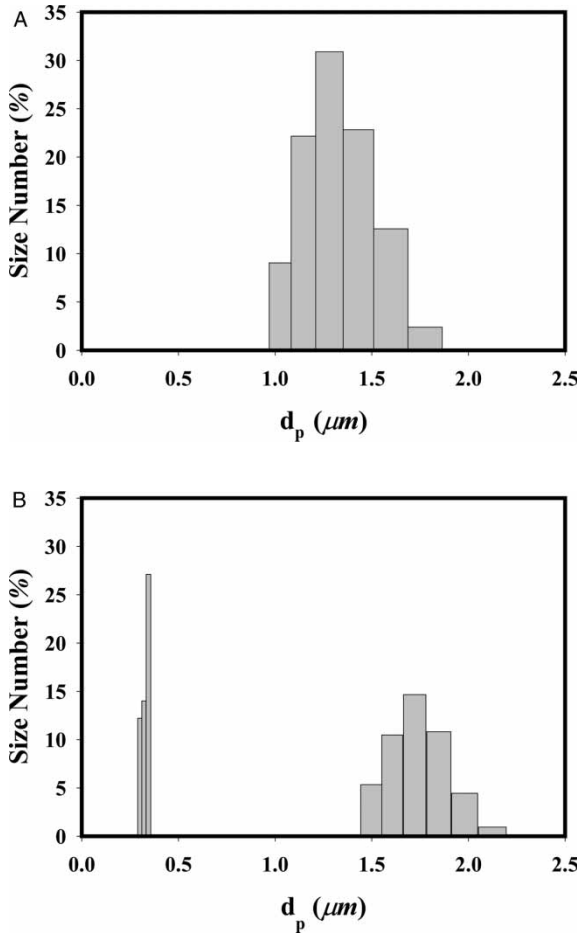

Figure 2. Particle distribution of (A) kaolin and (B) bentonite measured with a laser particle analyzer.

the flow could provide the desired mixing to bring the particles near the membrane surface into the bulk fluid. The groove for this study is of rectangular shape due to difficulty of fabrication. The width and the depth of the groove in the longitudinal direction are 4.5 and 2.3 mm, respectively. Details of the modules are summarized in Table 1.

Methods

A new membrane was loaded in the membrane module and then compacted with ultra-pure water at 2 bar which was at least 30% higher than the

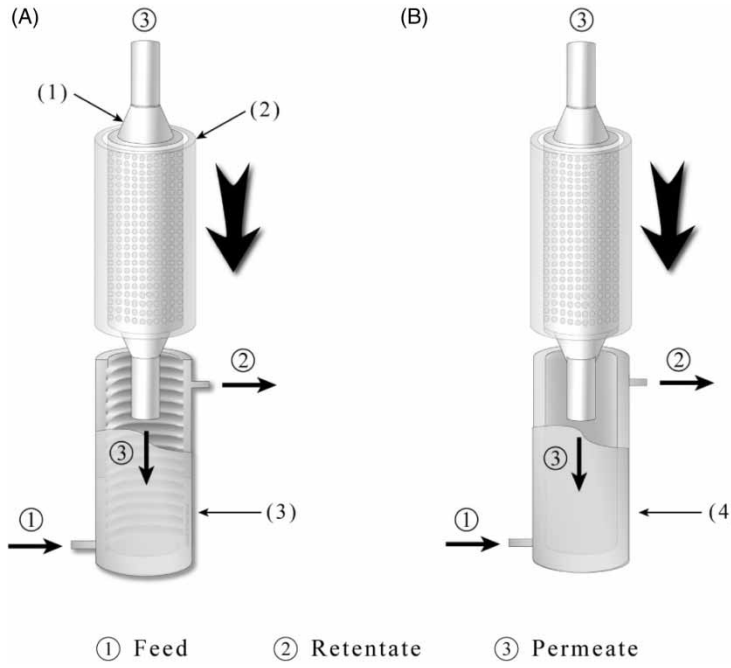

Figure 3. Details of the (A) helical and (B) flat type membrane modules: (1) perforated membrane support, (2) membrane, (3) cylinder with a helical groove and (4) cylinder.

maximum applied pressure used for the permeation experiments. The next step was to measure the initial water flux (J_{w1}) at the operating pressure. Fouling experiments for a solution containing particles were carried out at a given set of operating pressure, feed flow rate and concentration. Permeate data were taken every minute during the experiment. After each run, the membrane and apparatus were thoroughly cleaned using pre-filtered and ultra-pure water. The membrane housing,

Table 1. Helical and flat type membrane module configuration

	Helical type (mm)	Flat type (mm)
Cylinder inner radius (R_1)	20.0	21.8
Membrane support radius (R_2)	19.3	19.3
Flow channel width ($W = R_1 - R_2$)	0.7	2.5
Helical duct depth	2.3	—
Helical duct width	4.5	—
Helical duct pitch	0.4	—

either the helical groove or flat type, was then replaced and the fouling experiment was repeated at a given operating condition as described previously. Also, air could be injected at the entrance of the module by a compressor in order to measure the effect of air scouring and gas/liquid turbulent flow on gel layer deposit or membrane fouling. Finally, the pure water flux (J_{w2}) was measured again to evaluate the degree of the membrane fouling. The percentage of water flux recovery (J_{w2}/J_{w1}) was within $95 \pm 3\%$. All experiments were conducted at a temperature of $25 \pm 2^{\circ}C$. The particle rejection was measured with a turbidity meter (No. 8391-40, Cole Parmer Co.) and was greater than 95% for all experiments.

RESULTS AND DISCUSSION

Pressure Effect on Flux Enhancement

For each experiment the permeate fluxes were measured for flat ($J_{f,}$) and helical (J_h) modules in sequence. The membrane was always cleaned before the module was replaced. By keeping the operating pressure and flow rate the same for each membrane, it was possible to determine the effectiveness of vortices due to helical grooves by comparing J_h with J_f. Experimental data for 0.05 wt% kaolin and bentonite solutions at various operating pressures are shown in Fig. 4(A) and (B), respectively. The operating pressure was maintained below 1.5 bar because of experimental apparatus limitations. The feed flow rate was 2.0 L/min. The permeate fluxes for the kaolin solution were much higher than those for the bentonite solution. For all cases, significant flux declines were observed during the first 10 min, followed by a gradual stabilization of the flux. The flux declines for the helical module were significantly smaller than those observed for the flat module. The permeate fluxes for the two modules after 60 min are compared in Table 2. The flux enhancements observed with the helical module relative to the flat module for kaolin and bentonite solutions decreased from 25.0 and 24.9% to 5.9 and 0.8%, respectively, as the operating pressure increased to 1.5 bar. Increased operating pressure can provide an additional driving force for permeation flux, but it also can compress the cake layer. Hence, as the operating pressure increases, the beneficial wall shear force induced in the helical module may not be sufficient to prevent membrane fouling. Also, vortex flow in the helical module was more efficient in preventing flux decline for the kaolin solution, which exhibited higher permeate flux. Apparently, the cake resistance on the membrane surface for the kaolin solution was less than that for the bentonite solution (37), and the kaolin particles more easily transported away from the membrane by turbulent flow in the helical module.

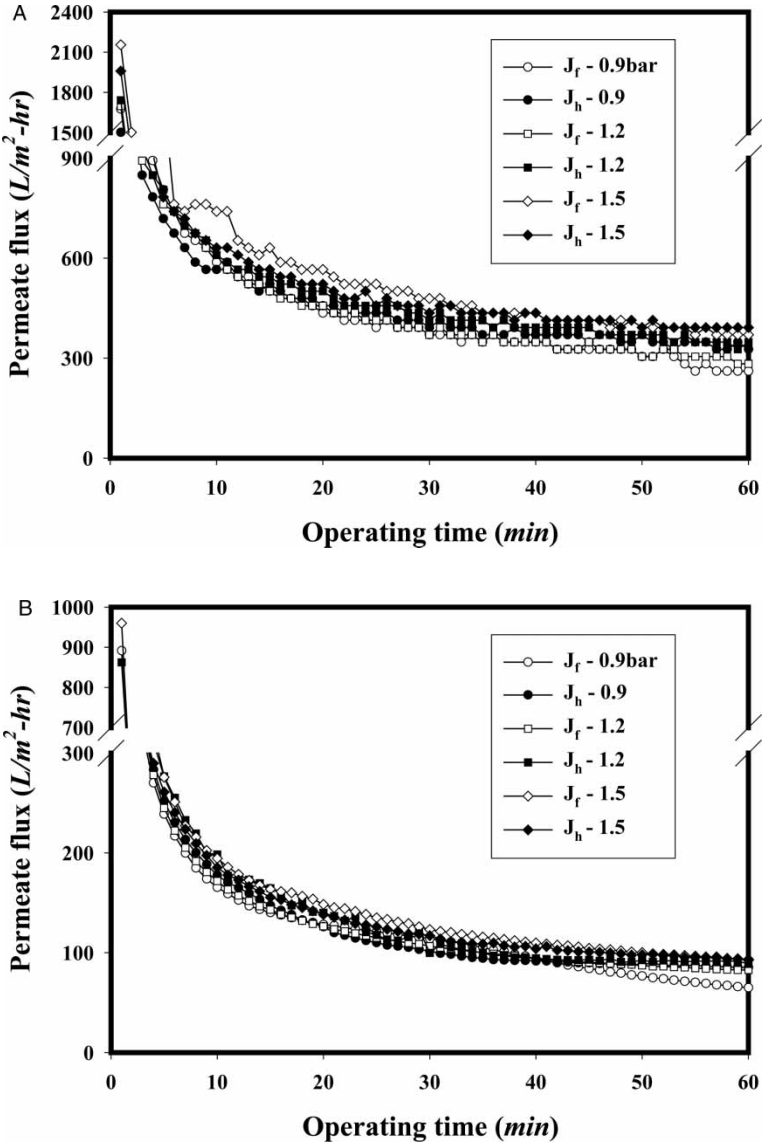

Figure 4. Permeate fluxes of the helical and flat modules as a function of operating pressure for (A) kaolin and (B) bentonite 0.05 wt% solutions at a flow rate of 2.0 L/min. J_f: permeate flux for flat module, J_h: permeate flux for helical module.

Feed Flow Rate Effect on Flux Enhancement

The effect of feed flow rate on flux enhancement by the helical module was investigated under fixed conditions of 0.05 wt% particle solution and a feed

Table 2. Permeate fluxes (L/m^2-hr) and flux enhancement for 0.05 wt% solution at various operating pressures and a feed flow rate of 2.0 L/min after the first hour of operation

	0.9 bar			1.2 bar			1.5 bar		
	Flat	Helical	F.E. (%)	Flat	Helical	F.E. (%)	Flat	Helical	F.E. (%)
Kaolin	261.2	326.5	25.0	304.8	348.3	14.3	370.1	391.8	5.9
Bentonite	65.0	81.2	24.9	82.7	88.8	7.4	92.7	93.4	0.8

F.E. = [(Helical − Flat)/Flat] × 100 %.

pressure of 1.2 bar. The permeate fluxes with respect to time for various flow rates of kaolin and bentonite are shown in Fig. 5(A) and (B), respectively. The permeate fluxes after 60 min are summarized in Table 3. There was not a significant effect of feed flow rate on the permeate flux enhancement for either kaolin or bentonite solutions. For both cases, the helical module exhibited higher permeate fluxes than the flat module. For example, the kaolin and bentonite flux enhancements obtained by using the helical module were 14.3 and 7.4% at 2.0 L/min, respectively, as shown in Table 3. As the feed flow rate increased to 3.0 L/min, there was not a significant change in flux enhancement.

Concentration Effect on Flux Enhancement

The effect of particle concentration on flux enhancement in the helical module was investigated under fixed conditions of 2 L/min feed flow rate and a feed pressure of 1.2 bar. The permeate fluxes with respect to time for various concentrations of kaolin and bentonite are shown in Fig. 6(A) and (B), respectively. Significant flux declines were observed during the first 10 min, followed by a progressive stabilization of the flux, similar to the dependence of water flux on pressure, as shown in Fig. 4(A) and (B). However, we observed that particle concentration affected the permeate flux more significantly than pressure and flow rate. The permeate flux decreased with increasing concentrations of the kaolin and bentonite solutions. The permeate fluxes after 60 min of operating time are summarized in Table 4. As the concentration of the feed solution increased, the amount of rejected kaolin particles increased, and they were packed closely near the membrane surface. A gel layer produced by the rejected particles provide significant resistances for water permeation through the membrane. However, it was observed that the helical and leakage flows induced by the helical module could effectively reduce the cake resistance on the membrane surface. The kaolin flux enhancements obtained by using the helical module under a low

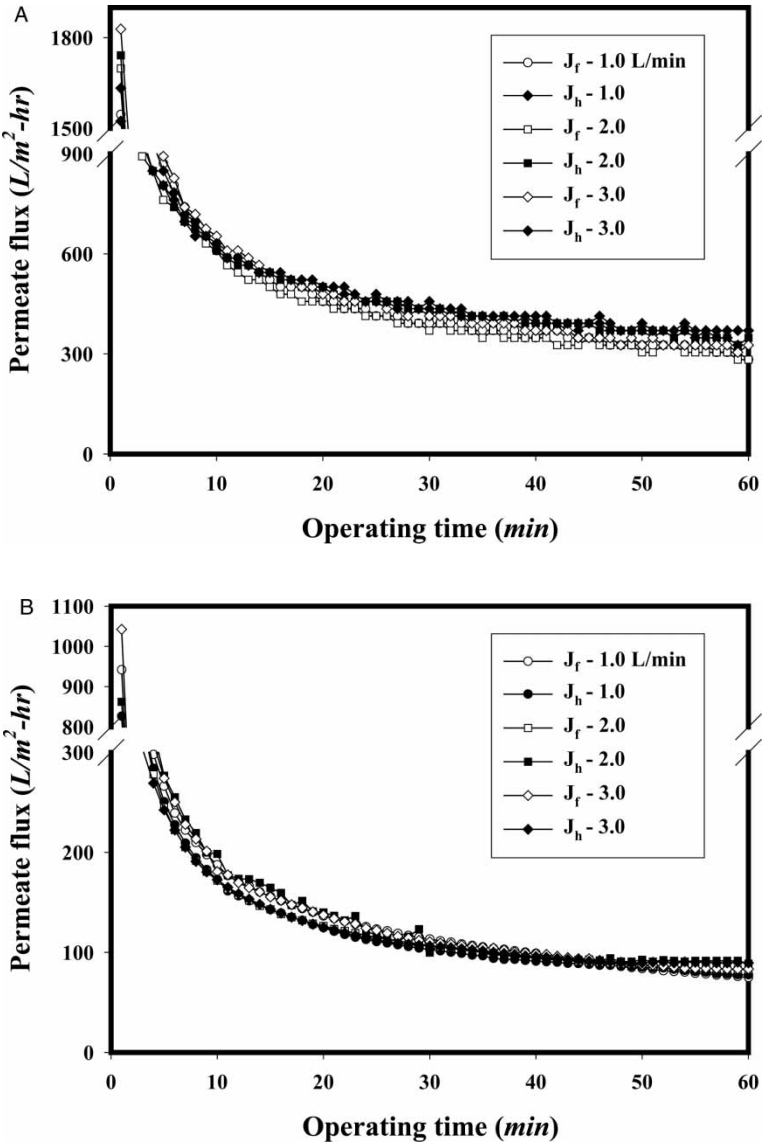

Figure 5. Permeate fluxes of the helical and flat modules as a function of feed flow rate for (A) kaolin and (B) bentonite 0.05 wt% solutions at 1.2. bar. J_f: permeate flux for flat module, J_h: permeate flux for helical module.

operating pressure of 1.2 bar increased from 14.3 to 57.2% as the kaolin concentration increased from 0.05 to 0.3 wt%. The flux enhancements for bentonite solutions were lower than those of kaolin solutions, but also

Table 3. Permeate fluxes (L/m^2-hr) and flux enhancement for 0.05 wt% solution at various feed flow rates and 1.2 bar after the first hour of operation

	1.0 L/min			2.0 L/min			3.0 L/min		
	Flat	Helical	F.E. (%)	Flat	Helical	F.E. (%)	Flat	Helical	F.E. (%)
Kaolin	283	326.5	15.4	304.8	348.3	14.3	326.5	370.1	13.4
Bentonite	74.9	77.5	3.5	82.7	88.8	7.4	83.4	89.5	7.3

increased with increasing particle concentration: 7.4 and 31.3% for 0.05 and 0.3 wt% bentonite solutions, respectively.

Effect of Gas Injection on Flux Enhancement

At first the liquid solution was fed to the membrane module by the feed pump. Then, the compressed air above 1.3 bar was injected and mixed with the liquid solution in front of the membrane module. The induced gas-liquid two-phase flow pattern corresponded to the ratio $r = U_g/(U_g + U_l)$ where U_g and U_l are the superficial gas and liquid velocities, respectively (38). The r was 0.4 for this experiment ($U_g = 1.3$ and $U_l = 2$ L/min at 1.3 bar). For $0.25 < r < 0.9$, large bubbles were observed, and called slug flow. This phenomenon induced a highly variable shear rate against the wall, and showed the most efficient regime for significant enhancement of mass flow (39). The permeate fluxes were measured for the flat module with and without air injection. Thereafter, the membrane module was dismantled. The used membrane was cleaned and reinstalled with the helical module instead of the flat module. The permeate flux was measured for the helical module in the same way as the flat module. In this way, the membrane testing conditions for the helical module experiment was very similar to that of the flat module experiment. The air flow rate was fixed at about 1.3 L/min under 1.3 bar because changing the air flow rate in our small system was difficult. The permeate flux for 0.1 wt% kaolin solution at 1.3 bar and a liquid flow rate of 2 L/min is shown in Fig. 7. In order to confirm the effect of the air injection the experiments were carried out with air injection during the first hour, without air injection during the second hour, and finally with air injection again during the last hour. Significant flux declines were observed during the first 10 min for both module types, followed by a progressive stabilization of the flux; however, the flux for the flat module declined significantly more than that of the helical module. The permeation fluxes of kaolin solution for the flat and helical modules after the first hour were 268.2 and 393.1 LMH, respectively. The flux enhancement for the helical module with air injection was 47% at the first hour. The fluxes for the flat and helical

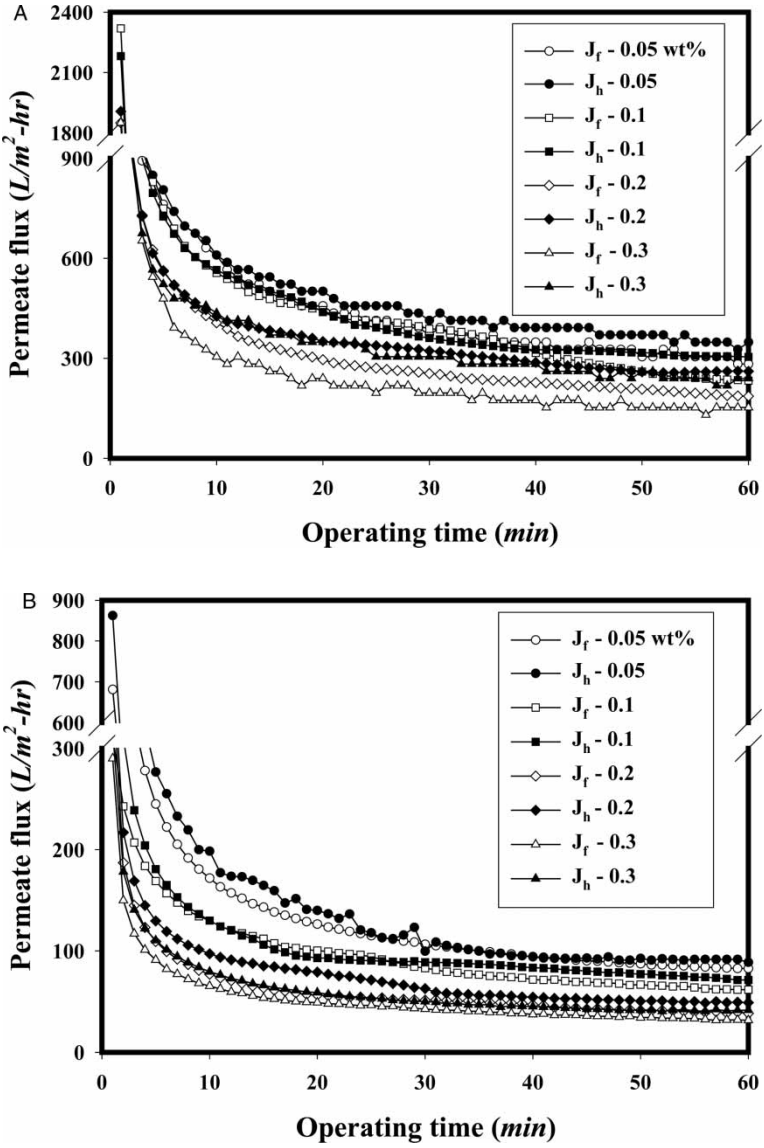

Figure 6. Permeate fluxes of the helical and flat modules as a function of feed concentration for (A) kaolin and (B) bentonite at 2.0 L/min and 1.2. bar. J_f: permeate flux for flat module, J_h: permeate flux for helical module.

modules decreased suddenly to 226.6 and 365.5 LMH, respectively, as soon as stopping the air injection. Then the fluxes for the flat and helical modules deceased gradually to 160.1 and 270.8 LMH, respectively, at the second hour. However, the fluxes for the flat and helical modules with air reinjection

Table 4. Permeate fluxes (L/m^2-hr) and flux enhancement at various feed concentrations at a feed pressure of 1.2 bar and feed flow rate of 2.0 L/min after the first hour of operation

	Kaolin	Bentonite
0.05wt%		
Flat	304.8	82.7
Helical	348.3	88.8
F.E. (%)	14.3	7.4
0.1wt%		
Flat	233.2	61.8
Helical	304.2	71.4
F.E. (%)	30.4	15.5
0.2wt%		
Flat	186.4	38.3
Helical	260.9	49.0
F.E. (%)	40	27.9
0.3wt%		
Flat	152.4	31.6
Helical	239.5	41.5
F.E. (%)	57.2	31.3

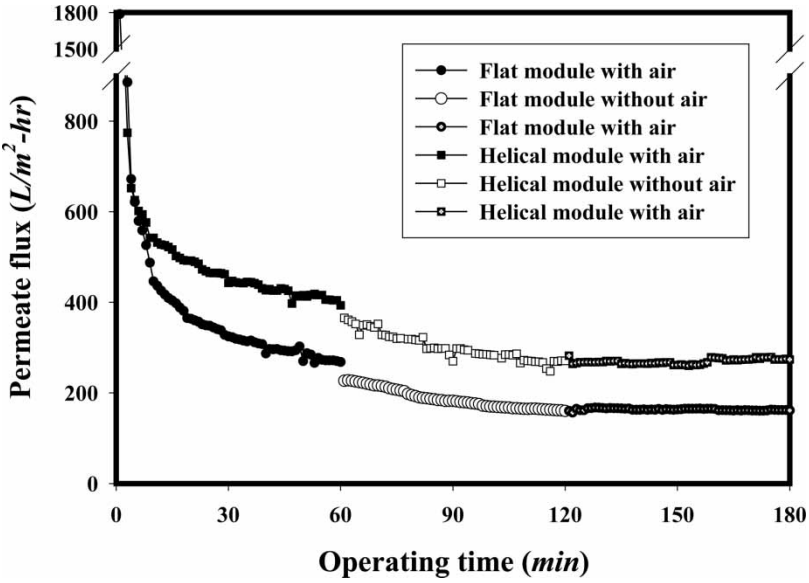

Figure 7. Permeate fluxes of the helical and flat modules with and without air injection for 0.1 wt% kaolin solution at 1.3. bar and 2.0 L/min.

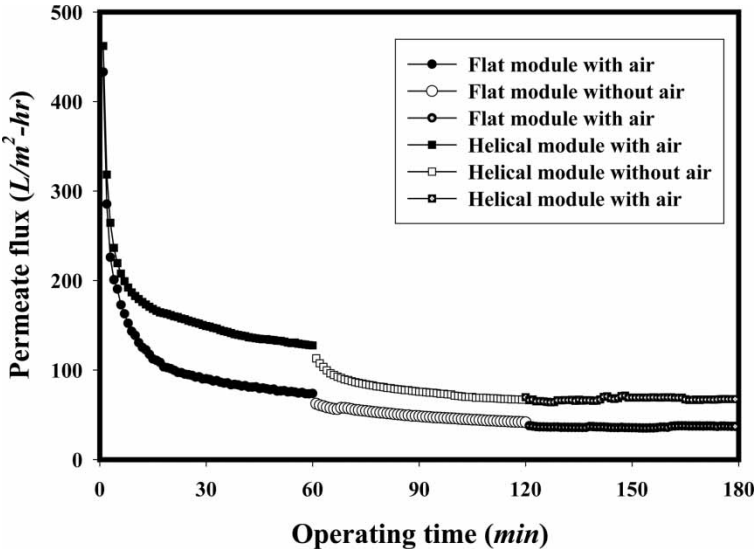

Figure 8. Permeate fluxes of the helical and flat modules with and without air injection for 0.1 wt% bentonite solution at 1.3. bar and 2.0 L/min.

were maintained within 1% variation during the last hour. The air injection was not efficient to destabilize the pre-existing cake deposit.

The permeate flux for 0.1 wt% bentonite solution at 1.3 bar and a liquid flow rate of 2 L/min is shown in Fig. 8. Significant flux declines were observed, qualitatively similar to the flux decline using kaolin-containing solutions. The permeation fluxes of bentonite solution for the flat and helical modules at the first hour were 73.7 and 127.6 LMH, respectively. The flux enhancement of bentonite solution for the helical module with air injection was 73%, which was 55% greater than that using kaolin. During the second hour the fluxes for the flat and helical modules deceased to 41.7 and 66.9 LMH, respectively. Significant effects of air sparging were observed for filtration of bentonite using the helical module by comparing the flux behavior during the second hour. The flux for the flat module with air reinjection decreased to 10%, but the flux for the helical module was maintained within 1% variation during the last hour. The flux enhancement for the helical module with air injection was significant. However, air injection to the system was not strong enough to completely remove a kaolin or bentonite cake layer formed on the membrane surface, even if air injection could maintain a constant flux after an operating time of 2 h. Consequently, air scouring strongly depended on the cake layer characteristics. Future studies should focus on the dependence of flux change with respect to the air injection conditions.

CONCLUSIONS

In this work, the effects of a helical module design with and without gas injection on permeate flux in microfiltration of kaolin and bentonite solutions were investigated and the following conclusions can be made:

(1) Centrifugal instabilities resulting from flow in helically grooved channels as well as the leakage flow between adjacent grooves generated secondary vortex flows and could reduce cake accumulation on the membrane surface. The permeation flux for the helical module without gas injection was 57% higher than that of the flat module for 0.3 wt% kaolin solution. This was the maximum flux enhancement obtained.
(2) The flux enhancement by the helical module for kaolin and bentonite solutions decreased as the operating pressure increased. In addition, vortex flow induced by the helical module was more effective at reducing membrane fouling for the case of kaolin filtration than that of bentonite. The feed flow rate as an operating parameter was not significant for either kaolin or bentonite solutions within experimental uncertainty.
(3) The flux enhancement for the helical module increased as kaolin or bentonite concentration in the feed increased.
(4) With gas injection, the fluxes for flat and helical modules were enhanced. The flux enhancement for the helical module with air injection was significant. For instance, the flux enhancements for kaolin and bentonite solutions using the helical module were 47 and 73%, respectively. However, the air injection conditions for the system were not strong enough to completely remove the pre-formed kaolin or bentonite cake layer on the membrane surface.

REFERENCES

1. Chung, K.Y., Brewster, M.E., and Belfort, G. (1998) Dean vortices with wall flux in a curved channel membrane system 3. *Concentration polarization in a spiral reverse osmosis slit. J. Chem. Eng. Japan*, 31 (5): 683–693.
2. Field, R.W., Wu, D., Howell, J.A., and Gupta, B.B. (1995) Critical flux concept for microfiltration fouling. *J. Membrane Sci.*, 100: 259–272.
3. Yamagishi, H., Crivello, J.V., and Belfort, G. (1995) Evaluation of photochemically modified poly(arylsulphone) ultrafiltration membranes. *J. Membrane Sci.*, 105: 249–259.
4. Copas, A. and Middleman, S. (1974) Use of convection promotion in the ultrafiltration of a gel-forming solute. *Ind. Eng. Chem., Process Des. Develop.*, 13 (2): 143–145.

5. Hiddink, J., Kloosterboer, D., and Bruin, S. (1980) Evaluation of static mixer as convective promoters in the ultrafiltration of dairy liquids. *Desalination*, 35: 149–167.
6. Najarian, S. and Bellhouse, B. (1996) Enhanced microfiltration of bovine blood using a tubular membrane with a screw-threaded insert and oscillatory flow. *J. Membrane Sci.*, 112: 249–261.
7. Kim, J.P., Kim, J.J., Chun, M.S., Min, B.R., and Chung, K.Y. (2001) Flux enhancement by glass balls inserted into a membrane module. *Water Sci. Tech.: Water Supply*, 1 (5/6): 285–292.
8. Takadono, S., Iwahori, H., Yabushita, T., and Imamura, Y. (1984) Treatment of highly fouling waste waters with tubular membrane systems. *Desalination*, 49: 347–355.
9. Rios, G.M., Rakotoarisoa, H., and Tarodo de la Fuente, B. (1987) Basic transport mechanisms of ultrafiltration in the presence of fluidized particles. *J. Membrane Sci.*, 34: 331–343.
10. Wang, Y., Howell, J., Field, R., and Wu, D. (1994) Simulation of cross-flow filtration for baffle tubular channels and pulsatile flow. *J. Membrane Sci.*, 95: 243–258.
11. Millward, H., Bellhouse, B., Sobey, I., and Lewis, R. (1995) Enhancement of plasma filtration using the concept of the vortex wave. *J. Membrane Sci.*, 100: 121–129.
12. Najarian, S. and Bellhouse, B. (1996) Effect of liquid pulsation on protein fractionation using ultrafiltration processes. *J. Membrane Sci.*, 114: 245–253.
13. Nuotila-Jokinen, J. and Nystrom, M. (1996) Comparison of membrane separation processes in the internal purification of paper mill water. *J. Membrane Sci.*, 119: 99–115.
14. Bouzerar, R., Jaffrin, M.Y., Ding, L.H., and Paullier, P. (2000) Influence of geometry and angular velocity on performance of a rotating disk filter. *AIChE J.*, 46 (2): 257–265.
15. Bouzerar, R., Paullier, P., and Jaffrin, M.Y. (2003) Concentration of mineral suspensions and industrial effluents using a rotating disk dynamic filtration module. *Desalination*, 158: 79–85.
16. Postlethwaite, J., Lamping, S.R., Leach, G.C., Hurwitz, M.F., and Lye, G.J. (2004) Flux and transmission characteristics of a vibrating microfiltration system operated at high biomass loading. *J. Membrane Sci.*, 228: 89–101.
17. Akoum, O., Jaffrin, M.Y., Ding, L.H., and Frappart, M. (2004) Treatment of dairy process waters using a vibrating filtration system and NF and RO membranes. *J. Membrane Sci.*, 235: 111–122.
18. Kroner, K.H., Nissinen, V., and Ziegler, H. (1987) Improved dynamic filtration of microbial suspensions. *Bio/technology*, 5: 921–926.
19. Belfort, G., Pimbley, J.M., Greiner, A., and Chung, K.Y. (1993) Diagnosis of membrane fouling using a rotating annular filter. 1. Cell culture media. *J. Membrane Sci.*, 77: 1–22.
20. Park, J.Y., Choi, C.K., and Kim, J.J. (1994) A study on dynamic separation of silica slurry using a rotating membrane filter 1. Experiments and filtrate fluxes. *J. Membrane Sci.*, 97: 1–22.
21. Lee, S.H. and Lueptow, R.M. (2004) Rotating membrane filtration and rotating reverse osmosis. *J. Chemical Eng. Japan.*, 37 (4): 471–482.
22. Winzeler, H.B. and Belfort, G. (1993) Enhanced performance for pressure-driven membrane processes: the argument for fluid instabilities. *J. Membrane Sci.*, 80: 35–47.

23. Chung, K.Y., Bate, R., and Belfort, G. (1993) Dean vortices with wall flux in a curved channel membrane system 4. Effect of vortices on permeation fluxes of suspensions in microporous membrane. *J. Membrane Sci.*, 81: 139–150.
24. Balakrishnan, M. and Agarwal, G. (1996) Protein fractionation in a vortex flow filter. I: Effect of system hydrodynamics and solution environment on single protein transmission. *J. Membrane Sci.*, 112: 47–74.
25. Mallubhotla, H., Nunes, E., and Belfort, G. (1995) Microfiltration of yeast suspensions with self-cleaning spiral vortices: possibilities for a new membrane module design. *Biotechol. Bioeng.*, 48: 375–385.
26. Moulin, P., Rouch, J., Serra, C., Clifton, M., and Aptel, P. (1996) Mass transfer improvement by secondary flows: Dean vortices in coiled tubular membranes. *J. Membrane Sci.*, 114: 235–244.
27. Mallubhotla, H., Hoffmann, S., Schmidt, M., Vente, J., and Belfort, G. (1998) Flux enhancement during Dean vortex tubular membrane nanofiltration. 10. Design, construction, and system characterization. *J. Membrane Sci.*, 141: 183–195.
28. Mallubhotla, H.H., Schmidt, M., Lee, K.H., and Belfort, G. (1999) Flux enhancement during Dean vortex tubular membrane nanofiltration. 13. Effects of concentration and solute type. *J. Membrane Sci.*, 153: 259–269.
29. Luque, S., Mallubhotla, H., Gehlert, G., Kuriyel, R., Dzengeleski, S., Pearl, S., and Belfort, G. (1999) A new coiled hollow-fiber module design for enhanced microfiltration performance in biotechnology. *Biotechol. Bioeng.*, 65: 247–257.
30. Kuakuvi, D.N., Moulin, P., and Charbit, F. (2000) Dean vortices: a comparison of woven versus helical and straight hollow fiber membrane modules. *J. Membrane Sci.*, 171: 59–65.
31. Ghogomu, J.N., Guigui, C., Rouch, J.C., Clifton, M.J., and Aptel, P. (2001) Hollow-fibre membrane module design: comparison of different curved geometries with Dean vortices. *J. Membrane Sci.*, 181: 71–80.
32. Bellhouse, B.J. (1997) Membrane filters with corkscrew vortex generating means. US Patent 5,628,909, May 13.
33. Muller, C.H., Agarwal, G.P., Melin, Th., and Wintgens, Th. (2003) Study of ultrafiltration of a single and binary protein solution in a thin spiral channel module. *J. Membrane Sci.*, 227: 51–69.
34. Cui, Z. and Wright, K. (1994) Gas-liquid two phase cross-flow ultrafiltration of BSA and dextran solutions. *J. Membrane Sci.*, 90: 183–189.
35. Cui, Z. and Wright, K. (1996) Flux enhancements with gas sparging in downwards crossflow ultrafiltration: performance and mechanism.. *J. Membrane Sci.*, 117: 109–116.
36. Um, M.J., Yoon, S.H., Lee, C.H., Chung, K.Y., and Kim, J.J. (2001) Flux enhancement with gas injection in crossflow ultrafiltration of oily wastewater. *Water Res.*, 35 (17): 4095–4101.
37. Chung, K.Y. (2001) Fouling characteristics in the microfiltration of mixed particle suspensions. *Membrane J.*, 11 (4): 161–169.
38. Vera, L., Villarroel, R., Delgado, S., and Elmaleh, S. (2000) Enhancing microfiltration through an inorganic tubular membrane by gas sparging. *J. Membrane Sci.*, 165: 47–57.
39. Cabassud, C., Laborie, S., and Laine, J.M. (1997) How slug flow can improve mass transfer in ultrafiltration organic hollow fibers. *J. Membrane Sci.*, 128: 93–101.